



OPEN ACCESS

# Reduced vessel density in deep capillary plexus correlates with retinal layer thickness in choroideremia

Alessandro Arrigo ,<sup>1</sup> Francesco Romano ,<sup>1,2</sup> Maurizio Battaglia Parodi,<sup>1</sup> Peter Charbel Issa,<sup>3,4</sup> Johannes Birtel,<sup>3,4,5</sup> Francesco Bandello ,<sup>1</sup> Robert E Maclaren<sup>6</sup>

<sup>1</sup>Department of Ophthalmology, Scientific Institute San Raffaele, University Vita-Salute, via Olgettina, 60, 20132, Milan, Italy

<sup>2</sup>Eye Clinic, Department of Biomedical and Clinical Science, Luigi Sacco University Hospital, Milano, Italy

<sup>3</sup>Oxford Eye Hospital, Oxford University Hospitals NHS Foundation Trust, Oxford, UK

<sup>4</sup>Nuffield Laboratory of Ophthalmology, Nuffield Department of Clinical Neurosciences, University of Oxford, Oxford, UK

<sup>5</sup>Department of Ophthalmology, University of Bonn, Bonn, Germany

<sup>6</sup>Oxford Eye Hospital, Oxford University Hospitals NHS Foundation Trust, and Nuffield Laboratory of Ophthalmology, Nuffield Department of Clinical Neurosciences, University of Oxford, Oxford, UK

## Correspondence to

Alessandro Arrigo, Department of Ophthalmology, IRCCS Ospedale San Raffaele, University Vita-Salute, Via Olgettina 60, Milan 20132, Italy; alessandro.arrigo@hotmail.com

Received 8 April 2020

Revised 19 May 2020

Accepted 29 May 2020

Published Online First 24 June 2020

## ABSTRACT

**Background** To assess retinal layer thickness in choroideremia (CHM) and to reveal its correlation with optical coherence tomography (OCT) angiography (OCTA) findings.

**Methods** The study was designed as an observational, cross-sectional clinical series of patients with CHM, which included 14 CHM eyes and 14 age-matched controls. Multimodal imaging included OCT and OCTA. The vessel density (VD) of superficial capillary (SCP), deep capillary (DCP) and choriocapillaris (CC) plexuses was analysed by OCTA. The apparently preserved retinal islet and atrophic regions were investigated separately. Main outcome measures were as follows: best-corrected visual acuity (BCVA), total retinal layers, ganglion cell layer (GCL), inner plexiform layer (IPL), inner nuclear layer (INL), outer plexiform layer (OPL), outer nuclear layer (ONL), ellipsoid zone–retinal pigment epithelium (EZ-RPE) layer, choroidal thickness and VDs of SCP, DCP and of CC.

**Results** Mean BCVA was 0.0±0.0 LogMAR in both groups. GCL, ONL, EZ-RPE and choroid were significantly thinned in CHM, particularly in the atrophic region. OPL was unaffected in the apparently preserved islet, whereas INL and IPL were similarly thinned in the atrophic and apparently preserved retina. DCP appeared severely affected in both regions, while CC was only altered in the atrophic retina. Significant correlations were found between OCT and OCTA parameters.

**Conclusions** Our study showed severe alterations in both outer and inner retinal layers of patients with CHM. The extended retinal involvement might be the consequence of neuronal and vascular trophic factor reduction produced by the primarily altered RPE and/or secondary Müller glial cell reaction.

degrees of photoreceptor and RPE degeneration in affected areas.<sup>6–10</sup> A loss of nuclei has been observed in the inner retina in postmortem tissue.<sup>8</sup>

Patients with CHM generally report nyctalopia in the first two decades of life, and the disease may lead to blindness in middle age.<sup>3,4</sup> However, since visual acuity does not deteriorate until the disease's late stages, anatomical endpoints may provide additional help in determining disease progression. Numerous ophthalmic imaging studies have studied morphological and functional alterations in CHM.<sup>11–19</sup> However, no study has thoroughly investigated quantitative alterations occurring in retinal layers.

The goal of this study was to assess retinal layer thickness in patients with CHM by performing measurements both in the apparently preserved central islet and in the atrophic retina, and to correlate these findings with optical coherence tomography (OCT) angiography (OCTA) data.

## MATERIALS AND METHODS

The study was designed as an observational, cross-sectional clinical series of patients with CHM. Patients and healthy controls were consecutively recruited from the Inherited Retinal Dystrophy Units at the Department of Ophthalmology, Scientific Institute San Raffaele, Milan, Italy, and the Department of Ophthalmology, University of Bonn, Germany. Written informed consent was obtained from all subjects, and the study adhered to the tenets of the Declaration of Helsinki. The study was approved by the Ethical Committee of Scientific Institute San Raffaele, Milan (NET-2016-02363765).

Inclusion criteria included (1) a genetically confirmed clinical diagnosis of CHM, (2) foveal sparing and (3) clear optical media. Exclusion criteria included (1) the presence of other retinal or optic nerve disorders, (2) cystoid macular oedema, (3) refractive errors greater than ±3 D, (4) previous ophthalmic surgery and systemic conditions potentially altering retinal anatomy and function. The control group did not reveal any ocular or systemic diseases, and was age-matched, sex-matched and ethnicity-matched with the patient group.

Both cohorts underwent a complete ophthalmologic examination, including best-corrected visual acuity (BCVA) testing, slit-lamp biomicroscopy, Goldmann applanation tonometry, funduscopy examination, colour fundus photography (TRC-50DX, Topcon Corporation; Tokyo, Japan, or

## INTRODUCTION

Choroideremia (CHM) is an X-linked recessive retinal disease characterised by gradual and centripetal chorioretinal degeneration, with the fundus having a typically pale end-stage appearance.<sup>1–4</sup> The disease is caused by mutations in the CHM gene that encodes the Rab escort protein-1, which interacts with Rab27a, an intracellular protein involved in protein prenylation and is believed to be necessary for vesicle trafficking in the retinal pigment epithelium (RPE).<sup>5</sup> Several histological reports carry images depicting the chorioretinal degeneration, including an independent choriocapillaris (CC), RPE and outer retina degeneration; areas of well-preserved retina in the vicinity of severe atrophy; and discordant



© Author(s) (or their employer(s)) 2021. Re-use permitted under CC BY-NC. No commercial re-use. See rights and permissions. Published by BMJ.

**To cite:** Arrigo A, Romano F, Parodi MB, et al. *Br J Ophthalmol* 2021;**105**:687–693.

Visucam, Zeiss, Oberkochen, Germany), blue-light fundus autofluorescence (BL-FAF) and spectral domain-OCT (SD-OCT; Spectralis HRA+OCT, Heidelberg Engineering; Heidelberg, Germany). A subgroup underwent 12×12-mm OCTA examination (DRI Triton OCT, Topcon Corporation; or PLEX Elite 9000, ZEISS, Dublin, California, USA). The acquisition protocol included a single-line SD-OCT acquisition (1024 A-scans per B-line scan; automatic real time (ART)=100 frames), passing through the fovea. Eye tracking was enabled during the examination. Two independent graders (FR and AA) measured retinal layers. In patients with CHM, measurements were performed at the point of maximal foveal thickness in the apparently preserved retina, within a 1.5 mm diameter area centred on the middle of the fovea, and 100 µm external to the boundary between the apparently preserved retina and the atrophic retina. In the controls, the thickest foveal site was evaluated. The following were assessed: total retinal layer, ganglion cell layer (GCL), inner plexiform layer (IPL), inner nuclear layer (INL), outer plexiform layer (OPL), outer nuclear layer (ONL) and ellipsoid zone-RPE(EZ-RPE) layer.<sup>20</sup> The mean of the two independent measurements from the same structural scan was used for the statistical analysis. The areas of apparently preserved retina were outlined on the BL-FAF image. On OCTA, vessel densities (VDs) from the superficial capillary (SCP), deep capillary (DCP) and CC) plexuses were independently quantified in the apparently preserved and in the atrophic areas, using a previously validated method.<sup>18 21 22</sup> The images were loaded in the Fiji software package<sup>23</sup> and binarised using a mean threshold, together with the following pipeline: Image -> Adjust -> Automatic Threshold -> Mean threshold. In-house scripts were then used to calculate the ratio between white and black pixels in the manually segmented foveal avascular zone, introducing exclusion criteria.

The primary outcome measure was the assessment of the retinal layer status. Secondary outcomes included their correlations with the extent of the degenerative lesion and of the vascular alterations.

Differences in thickness were studied by means of analysis of variance for repeated measures and Bonferroni's correction for posthoc analysis. The relationship between morphological and epidemiological variables was explored using Kendall's Tau-b (non-parametric) correlation test. Results for descriptive analyses are expressed as mean±SD for quantitative values and as frequency and percentages for categorical ones. Interobserver reproducibility for the measurement of all the different layers was evaluated by means of intraclass correlation coefficients (95% CIs). Statistical significance was set at  $p < 0.05$ , with all the analyses being performed using the SPSS Statistics Version 21.0 Software package (IBM; Armonk, New York, USA).

## RESULTS

Overall, 14 patients with CHM (14 eyes) and 14 healthy male controls were included. Mean age was  $38.2 \pm 8.9$  years (range: 23–56; median: 36) and  $35.3 \pm 8.2$  (range: 27–51; median: 36) for patients and controls, respectively. LogMAR BCVA was  $0.0 \pm 0.0$  for both groups. No differences in age, ethnicity or intraocular pressure were observed (all  $p > 0.05$ ). A specimen case of CHM is shown in figure 1.

Statistical analysis revealed significant retinal and choroidal thinning in patients with CHM compared with controls ( $F = 160.8$  and  $135.6$ , respectively; both  $p < 0.001$ ). Quantitative measurement of total retinal thickness revealed a thinner retina in patients with CHM compared with controls (both  $p < 0.001$ ), not only in the atrophic region but also in the apparently preserved retina. Considering retinal layers separately, the thinning of the GCL, ONL, EZ-RPE and choroid (all  $p < 0.01$ ) was more pronounced in the atrophic region compared with the apparently preserved central islet. In contrast, OPL thickness within the apparently preserved central islet of patients with CHM did not differ with respect to the controls ( $p = 0.88$ ) but was significantly thinner in the atrophic region (both  $p < 0.001$ ). INL thickness was significantly reduced both in the atrophic region and in the apparently preserved islet, when compared with controls (both

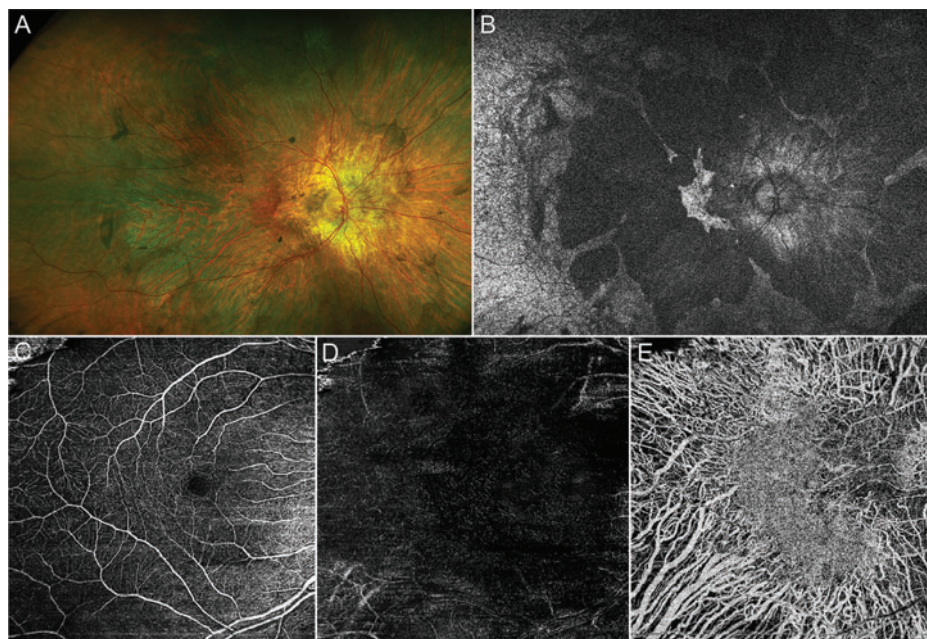


**Figure 1** Multimodal fundus imaging features in choroideremia. Colour and fundus autofluorescence images (A,B) show extensive retinal atrophy, with the sparing of a central retinal islet. OCTA analysis reveals preserved SCP (C), remarkably altered DCP (D) and total loss of CC, with preservation of the central islet region (E). CC, choriocapillaris; DCP, deep capillary; OCTA, optical coherence tomography angiography; SCP, superficial capillary.

**Table 1** Retinal layer thickness in patients with CHM and healthy controls

Retinal layer thickness							
CHM apparently preserved retinal islet							
EZ-RPE*	ONL*	OPL	INL*	IPL*	GCL*	RETINA*	CHOROID*
44.58±5.13	70.63±12.79	40.25±7.30	37.17±9.78	37.38±9.59	49.54±9.70	286.50±31.51	155.67±46.74
p<0.001	p<0.001	p>0.05	p<0.001	p<0.001	p<0.001	p<0.001	p<0.001
CHM atrophic retina							
EZ-RPE*	ONL*	OPL*	INL*	IPL*	GCL*	RETINA*	CHOROID*
21.96±3.38	37.67±14.32	30±9.73	36.75±9.05	37.71±7.93	40.75±9.97	217.88±36.87	75.96±34.05
p<0.001	p<0.001	p<0.001	p<0.001	p<0.001	p<0.001	p<0.001	p<0.001
Healthy controls							
EZ-RPE	ONL	OPL	INL	IPL	GCL	RETINA	CHOROID
72.81±5.55	92.13±7.24	41.13±5.89	45.94±6.33	47.75±7.06	61.86±7.39	398.24±18.57	286.86±91.15

All values are expressed in  $\mu\text{m}$  (mean±SD).

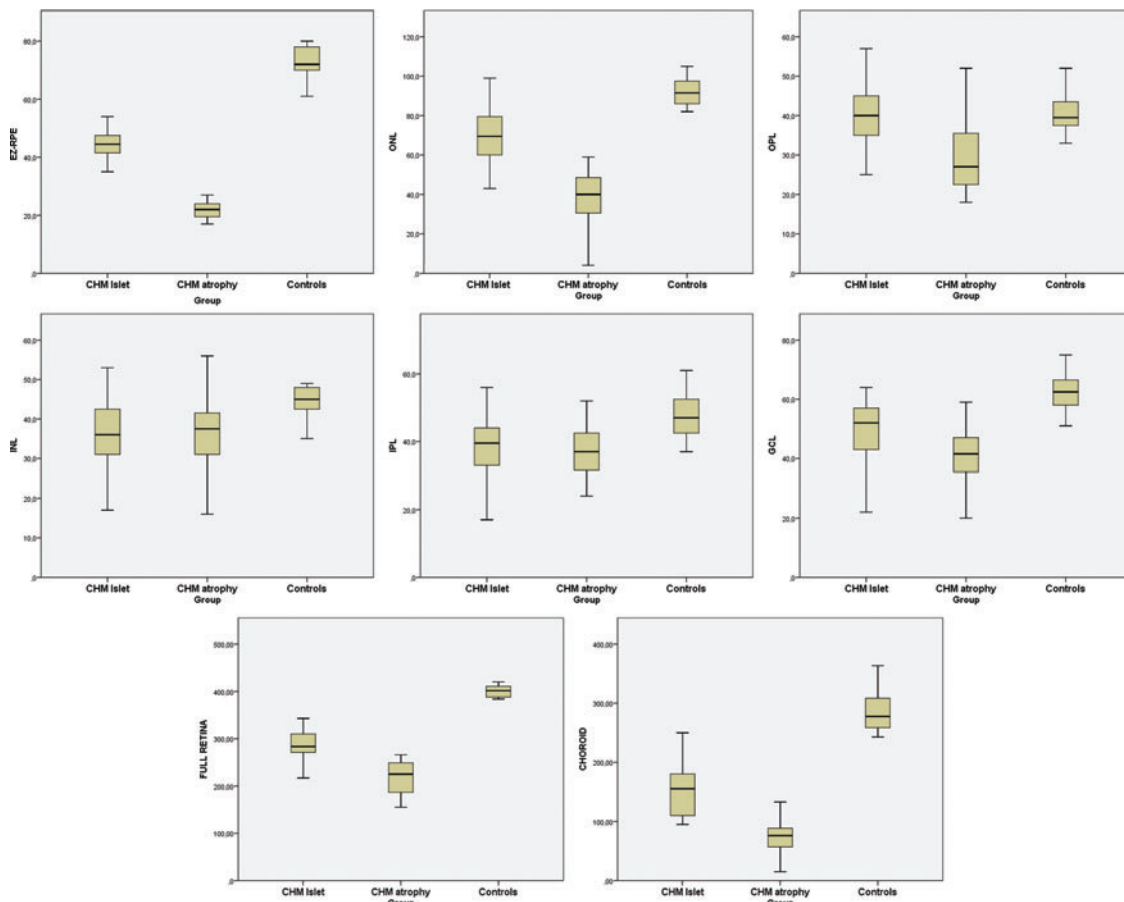
\*Statistically significant changes compared with controls.

CHM, choroideremia; EZ-RPE, ellipsoid zone–retinal pigment epithelium layer; GCL, ganglion cell layer; INL, inner nuclear layer; IPL, inner plexiform layer; ONL, outer nuclear layer; OPL, outer plexiform layer.

$p<0.01$ ), with no difference between the two CHM regions ( $p=0.89$ ). The IPL showed the same behaviour as the INL, with a comparable thinning in the atrophic retina and in the apparently preserved region ( $p=0.88$ ). All values are shown in [table 1](#) and [figure 2](#). Structural OCTs of retinal layers are shown in [figure 3](#).

OCTA analysis was performed in 11 of 14 patients (11 eyes included) and in all control subjects. In detail, seven eyes were examined by Topcon OCTA, whereas four eyes were analysed

using Zeiss OCTA. Significant differences between patients with CHM and controls were detected when measuring VD of DCP and of CC ( $F=3941.3$  and  $655.9$ , respectively; both  $p<0.001$ ). In contrast, SCP did not show VD alterations ( $p=0.90$ ). Considering the atrophic region and the apparently preserved islet independently, DCP VD was significantly lower both in the atrophic and in the apparently preserved retina compared with controls ( $p<0.001$ ). On the other hand, CC appeared to be altered only in the atrophic region ( $p<0.001$ ), and not in the

**Figure 2** Boxplots of retinal layer thickness in choroideremia.

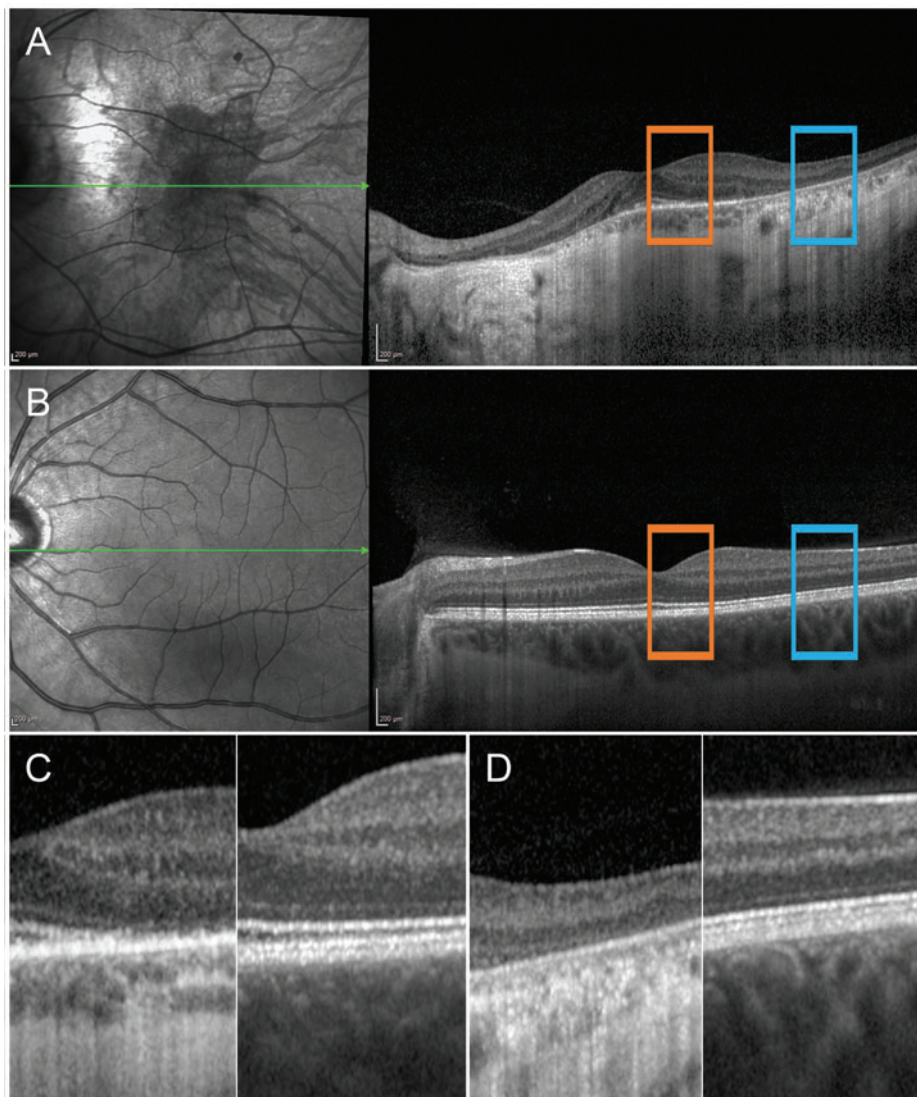


**Figure 3** Retinal layers in choroideremia. A specimen choroideremia case is shown in (A) and is compared with a control case (B). More specifically, retinal layers of the apparently preserved islet (orange squares and C) are found to be already remarkably altered in terms of thickness and reflective signal attenuation, compared with the control. The loss of normal morphological integrity is particularly evident in the atrophic region (blue squares and D).

apparently preserved islet ( $p=0.19$ ). SCP was unaffected in both regions ( $p>0.05$ ) (figure 4). All values are reported in table 2.

Interestingly, significant correlations were found between VD of DCP and the following retinal layers: OPL, INL, IPL. The complete correlation panel is shown in table 3.

## DISCUSSION

The present study assesses retinal layers both in the apparently preserved central islet and in the atrophic region. Their relationship with vascular impairment, detected on OCTA, is also considered. As expected, the atrophic retina appeared thinner, both globally and in relation to individual retinal layers. Significant differences between the apparently preserved central islet and the atrophic region were detected not only at the level of EZ-RPE and ONL but also in the inner retina (INL and IPL). These alterations were not confined to the atrophic retina but extended to the apparently preserved central islet. The EZ-RPE, ONL, INL, IPL and GCL were all markedly thinner than in the controls. It is notable that while INL and IPL showed the same degree of

thinning between the apparently preserved islet and the atrophic retina, the other retinal layers were characterised by an intermediate thinning in the apparently preserved islet.

Previous structural OCT investigations have described precise anatomical correspondences in the affected retina of patients with CHM between RPE degeneration and photoreceptor loss, including the ONL, the external limiting membrane and the EZ.<sup>13 14 17</sup> Moreover, OCTA has recently shown that profound alterations occur in the retinal vascular networks of these patients<sup>18</sup>; indeed, the DCP turned out to be almost completely absent both in the central apparently preserved islet and in the peripheral atrophic retina, whereas the CC was significantly altered only in the degenerated region. SCP was not significantly altered either in the apparently preserved islet or in the atrophic retina.

Interpreting the OCT and OCTA findings is a challenge. Bearing in mind the ubiquitous expression of the CHM gene across different cellular subtypes,<sup>17 24</sup> the well-known RPE degeneration may coexist with the inner retinal cell degeneration.

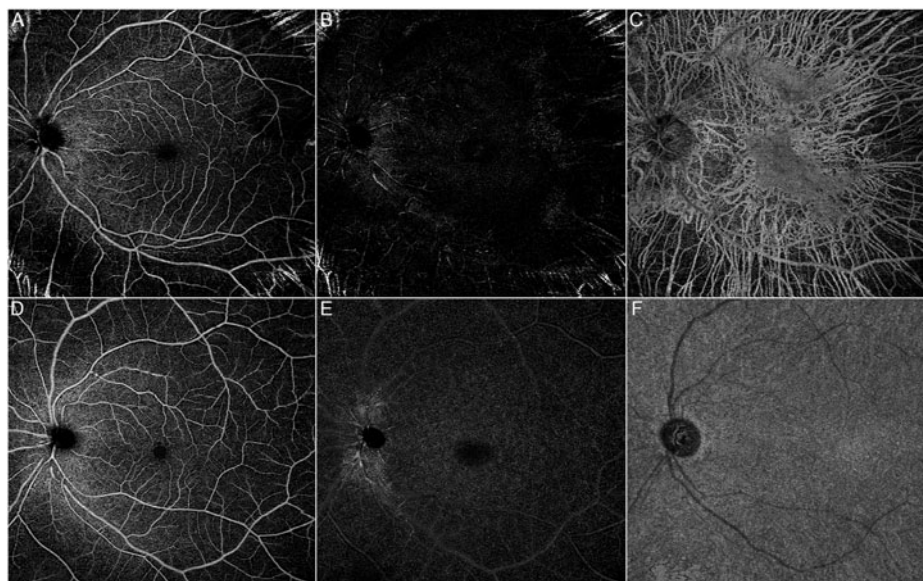


**Figure 4** OCTA features in choroideremia. A specimen choroideremia case shows the differences in SCP (A), DCP (B) and CC (C) compared with a healthy control (D, E, F, respectively). CC, choriocapillaris; OCTA, optical coherence tomography angiography; SCP, superficial capillary.

**Table 2** Vessel density analysis in patients with CHM and healthy controls

Vessel density analysis		
<b>CHM mean vessel density values</b>		
<b>SCP</b>	<b>DCP</b>	<b>CC</b>
0.412±0.014	0.017±0.009*	0.246±0.007*
p>0.05	p<0.001	p<0.001
<b>CHM apparently preserved islet vessel density values</b>		
<b>SCP</b>	<b>DCP*</b>	<b>CC</b>
0.413±0.021	0.020±0.013	0.492±0.015
p>0.05	p<0.001	p<0.001
<b>CHM atrophic retina vessel density values</b>		
<b>SCP</b>	<b>DCP*</b>	<b>CC*</b>
0.411±0.013	0.014±0.009	0.0±0.0
p>0.05	p<0.001	p<0.001
<b>Healthy controls</b>		
<b>SCP</b>	<b>DCP</b>	<b>CC</b>
0.425±0.026	0.432±0.027	0.501±0.024

All values are expressed in  $\mu\text{m}$  (mean±SD)

\*Statistically significant changes compared with controls.

CC, choriocapillaris; CHM, choroideremia; DCP, deep capillary; SCP, superficial capillary.

Our comprehensive hypothesis suggests an early impairment of RPE and Müller cells,<sup>25</sup> leading to a diminished production of the angiogenic and trophic factors that are essential to guarantee both vascular and neuronal integrity. As a consequence, the downregulation and reduced release of cytokines and growth factors may bring about the apoptosis of ganglion, amacrine and bipolar cells, as already found in other diseases.<sup>26–27</sup> This phenomenon might thus explain our findings regarding the reduction of INL, IPL and GCL thickness.

In addition, it should be noted that the decreased VD of DCP found both in the apparently preserved and in the atrophic regions might be explained by the inner retinal involvement of these regions. A DCP perfusion deficit might

be due to a self-regulating mechanism occurring secondary to the loss of the outer retinal layers, the latter leading to a drop in hypoxic drive and therefore reduced DCP perfusion speed or capillary loss. Furthermore, bearing in mind the primary role of the outer retina, our findings regarding the involvement of the inner retina might also be the consequence of a trans-synaptic degeneration. In addition, the possible impairment of other retinal cytotypes, especially the Müller cells, might lead to a loss of homeostasis and a reduction in the release of growth factors and other mediators.

In view of the recent rapid developments in CHM therapy, it is essential to develop biomarkers for the disease's progression, prognosis, inclusion into clinical trials and as an aid in improving surgical techniques.<sup>28–30</sup> We hypothesise that inner retina alterations may occur relatively early during the disease and might affect the outcome of the treatment adopted.

We acknowledge that our study has several limitations, including the intrinsic drawbacks of OCT-based techniques. Equally, although CHM is a rare condition, we realise the small number of patients contributes considerably to the research's weak statistical power. Moreover, the cross-sectional analysis of patients in advanced stages makes it impossible to determine when OCT and OCTA changes occur. We analysed patients displaying the classic manifestation of CHM in order to obtain the most uniform information about this choroidal degeneration. The use of two different swept-source OCTAs may be considered a further limitation. Although we found the data obtained from the two instruments to match, in accordance with a previous paper comparing different OCTA devices,<sup>31</sup> we recommend that OCTA findings generated by different devices be interpreted with care. For all the above-mentioned reasons, further studies are needed in order to validate microstructural retinal damage, as well as to test the effectiveness of OCT-based assessment and monitoring in CHM.

In conclusion, the present study demonstrates that neurosensory retinal alterations are not limited to the outer retina, but extend to the inner retinal layers, both in the atrophic and in the apparently preserved areas in patients with CHM. Further longitudinal studies are warranted in order to better characterise the degenerative course of the disease.

**Table 3** Correlation analysis of quantitative parameters in CHM

Correlation analysis							
<b>OPL_islet</b>	Parameter	<b>INL_islet</b>	<b>IPL_islet</b>	<b>RETINA_islet</b>	<b>ONL_atrophy</b>	<b>DCP_global</b>	<b>DCP_islet</b>
	Tau coefficient	0.626	0.651	0.452	0.428	0.625	0.851
	P value	0.00039	0.00025	0.0097	0.015	0.00035	1.14E-06
<b>INL_islet</b>	Parameter	<b>IPL_islet</b>	<b>RETINA_islet</b>	<b>CHOROID_islet</b>	<b>ONL_atrophy</b>	<b>DCP_global</b>	<b>DCP_islet</b>
	Tau coefficient	0.493	0.576	0.399	0.42	0.563	0.735
	P value	0.005	0.0009	0.022	0.016	0.001	0.000025
<b>IPL_islet</b>	Parameter	<b>CHOROID_islet</b>	<b>EZ-RPE_atrophy</b>	<b>ONL_atrophy</b>	<b>DCP_global</b>	<b>DCP_islet</b>	
	Tau coefficient	0.375	0.374	0.517	0.473	0.607	
	P value	0.033	0.038	0.0033	0.007	0.0005	
<b>GCL_islet</b>	Parameter	<b>RETINA_islet</b>					
	Tau coefficient	0.361					
	P value	0.039					
<b>RETINA_islet</b>	Parameter	<b>DCP_islet</b>					
	Tau coefficient	0.464					
	P value	0.007					
<b>CHOROID_islet</b>	Parameter	<b>EZ-RPE_atrophy</b>	<b>RETINA_atrophy</b>				
	Tau coefficient	0.402	0.559				
	P value	0.024	0.0013				
<b>ONL_atrophy</b>	Parameter	<b>DCP_global</b>	<b>DCP_islet</b>				
	Tau coefficient	0.48	0.507				
	P value	0.006	0.003				
<b>OPL_atrophy</b>	Parameter	<b>CHOROID_atrophy</b>					
	Tau coefficient	0.374					
	P value	0.035					
<b>INL_atrophy</b>	Parameter	<b>DCP_global</b>	<b>DCP_atrophy</b>				
	Tau coefficient	0.372	0.433				
	P value	0.033	0.0133				
<b>RETINA_atrophy</b>	Parameter	<b>DCP_global</b>	<b>DCP_islet</b>				
	Tau coefficient	0.341	0.341				
	P value	0.048	0.048				
<b>SCP_global</b>	Parameter	<b>SCP_islet</b>	<b>SCP_atrophy</b>				
	Tau coefficient	0.682	0.651				
	P value	0.000013	0.006				
<b>DCP_global</b>	Parameter	<b>DCP_islet</b>	<b>DCP_atrophy</b>				
	Tau coefficient	0.686	0.367				
	P value	0.00007	0.034				
<b>CC_global</b>	Parameter	<b>CC_islet</b>					
	Tau coefficient	0.724					
	P value	0.00003					

All the reported correlations proved statistically significant.

CC, choriocapillaris; CHM, choroideremia; DCP, deep capillary; EZ-RPE, ellipsoid zone–retinal pigment epithelium layer; GCL, ganglion cell layer; INL, inner nuclear layer; IPL, inner plexiform layer; ONL, outer nuclear layer; OPL, outer plexiform layer; SCP, superficial capillary.

**Contributors** AA and FR were involved in study design, data analysis, data interpretation and manuscript draft. PCI and JB were involved in data acquisition, data analysis and manuscript revision. MBP, FB and REM were involved in data interpretation, manuscript revision, study supervision.

**Funding** This study was supported by the National Institute of Health Research (NIHR) Oxford Biomedical Research Centre (BRC). The views expressed are those of the authors and not necessarily those of the NHS, the NIHR or the Department of Health. This work was supported by the Dr. Werner Jackstädt Foundation, Wuppertal, Germany (Grant S0134-10.22 to JB). Francesco Bandello is a consultant for Alcon (Fort Worth, Texas, USA), Alimera Sciences (Alpharetta, Georgia, USA), Allergan (Irvine, California, USA), Farmila-Thea (Clermont-Ferrand, France), Bayer Shering-Pharma (Berlin, Germany), Bausch + Lomb (Rochester, New York, USA), Genentech (San Francisco, California, USA), Hoffmann-La-Roche (Basel, Switzerland), Novagali Pharma (Évry, France), Novartis (Basel, Switzerland), Sanofi-Aventis (Paris, France), Thrombogenics (Heverlee, Belgium), Zeiss (Dublin, USA). Peter Charbel Issa is a

consultant for Gyroscope and receives research support from Heidelberg Engineering. Robert MacLaren is a consultant to Biogen (Boston, USA).

**Competing interests** None declared.

**Data sharing statement** No data are available.

**Provenance and peer review** Not commissioned; externally peer reviewed.

**Open access** This is an open access article distributed in accordance with the Creative Commons Attribution Non Commercial (CC BY-NC 4.0) license, which permits others to distribute, remix, adapt, build upon this work non-commercially, and license their derivative works on different terms, provided the original work is properly cited, appropriate credit is given, any changes made indicated, and the use is non-commercial. See: <http://creativecommons.org/licenses/by-nc/4.0/>.

**ORCID iDs**

Alessandro Arrigo <http://orcid.org/0000-0003-4715-8414>

Francesco Romano <http://orcid.org/0000-0002-0458-9727>  
 Francesco Bandello <http://orcid.org/0000-0003-3238-9682>

## REFERENCES

- MacDonald IM, Sereda C, McTaggart K, *et al.* Choroideremia gene testing. *Expert Rev Mol Diagn* 2004;4:478–84.
- Choroideremia KJ. A clinical and genetic study of 84 Finnish patients and 126 female carriers. *Acta Ophthalmol Suppl* 1986;176:1–68.
- Roberts MF, Fishman GA, Roberts DK, *et al.* Retrospective, longitudinal, and cross sectional study of visual acuity impairment in choroideraemia. *Br J Ophthalmol* 2002;86:658–62.
- Chan SC, Bubela T, Dimopoulos IS, *et al.* Choroideremia research: report and perspectives on the second International Scientific Symposium for Choroideremia. *Ophthalmic Genet* (2016);6810(May):1–9.
- Zinkernagel MS, MacLaren RE. Recent advances and future prospects in choroideremia. *Clin Ophthalmol* 2015;9:2195–200.
- McCulloch JC. The pathologic findings in two cases of choroideremia. *Trans Am Acad Ophthalmol Otolaryngol* 1950;54:565–72.
- Rafuse EV, Choroideremia MC. A pathological report. *Can J Ophthalmol* 1968;3:347–52.
- MacDonald IM, Russell L, Chan CC. Choroideremia: new findings from ocular pathology and review of recent literature. *Surv Ophthalmol* 2009;54:401–7.
- Rodrigues MM, Ballantine EJ, Wiggert BN, *et al.* Choroideremia: a clinical, electron microscopic, and biochemical report. *Ophthalmology* 1984;9:873–83.
- Cameron JD, Fine BS, Shapiro I. Histopathologic observations in choroideremia with emphasis on vascular changes of the uveal tract. *Ophthalmology* 1987;94:187–9612.
- Al-Qahtani AA, Ba-Ali S, Alabduljalil T, *et al.* Scleral pits in choroideremia: implications for retinal gene therapy. *Retina* 2018;38:1725–30.
- Abbouda A, Dubis AM, Webster AR, *et al.* Identifying characteristic features of the retinal and choroidal vasculature in choroideremia using optical coherence tomography angiography. *Eye (Lond)* 2018;32:563–71.
- Jolly JK, Xue K, Edwards TL, *et al.* Characterizing the natural history of visual function in choroideremia using microperimetry and multimodal retinal imaging. *Invest Ophthalmol Vis Sci* 2017;58:5575–83.
- Abbouda A, Lim WS, Sprogyte L, *et al.* Qualitative features of spectral-domain optical coherence tomography provide prognostic indicators for visual acuity in patients with choroideremia. *Ophthalmic Surg Lasers Imaging Retina* 2017;48:711–6.
- Hariri AH, Velaga SB, Girach A, *et al.* Measurement and reproducibility of preserved ellipsoid zone area and preserved retinal pigment epithelium area in eyes with choroideremia. *Am J Ophthalmol* 2017;179:110–17.
- Morgan JJ, Han G, Klinman E, *et al.* High-resolution adaptive optics retinal imaging of cellular structure in choroideremia. *Invest Ophthalmol Vis Sci* 2014;55:6381–97.
- Xue K, Oldani M, Jolly JK, *et al.* Correlation of optical coherence tomography and autofluorescence in the outer retina and choroid of patients with choroideremia. *Invest Ophthalmol Vis Sci* 2016;57:3674–84.
- Battaglia Parodi M, Arrigo A, MacLaren RE, *et al.* Vascular alterations revealed with optical coherence tomography angiography in patients with choroideremia. *Retina* 2019;39:1200–5.
- Birtel J, Salvetti AP, Jolly JK, *et al.* Near-infrared autofluorescence in choroideremia: anatomic and functional correlations. *Am J Ophthalmol* 2019;199:19–27.
- Invernizzi A, Pellegrini M, Acquistapace A, *et al.* Normative data for retinal-layer thickness maps generated by spectral-domain OCT in a white population. *Ophthalmol Retina* 2018;0:0.
- Battaglia Parodi M, Rabiolo A, Cicinelli MV, *et al.* Quantitative analysis of optical coherence tomography angiography in adult-onset foveomacular vitelliform dystrophy. *Retina* 2018;38:237–44.
- Battaglia Parodi M, Romano F, Cicinelli MV, *et al.* Retinal vascular impairment in best vitelliform macular dystrophy assessed by means of optical coherence tomography angiography. *Am J Ophthalmol* 2018;187:61–70.
- Schindelin J, Arganda-Carreras I, Frise E, *et al.* Fiji: an open-source platform for biological-image analysis. *Nat Methods* 2012;9:676–82.
- Gutkowska M, Ayuso C. Rab escort protein 1 (REP1) in intracellular traffic: a functional and pathophysiological overview. *Ophthalmic Genet* 2004;25:101–10.
- Jacobson SG, Cideciyan AV, Sumaroka A, *et al.* Remodeling of the human retina in choroideremia: rab escort protein 1 (REP-1) mutations. *Invest Ophthalmol Vis Sci* 2006;47:4113–20.
- Park HY, Kim JH, Park CK. Neuronal cell death in the inner retina and the influence of vascular endothelial growth factor inhibition in a diabetic rat model. *Am J Pathol* 2014;184:1752–62.
- Le YZ. VEGF production and signaling in Müller glia are critical to modulating vascular function and neuronal integrity in diabetic retinopathy and hypoxic retinal vascular diseases. *Vision Res* 2017;139:108–14.
- MacLaren RE, Groppa M, Barnard AR, *et al.* Retinal gene therapy in patients with choroideremia: initial findings from a phase 1/2 clinical trial. *Lancet* 2014;383:1129–37.
- Edwards TL, Jolly JK, Groppa M, *et al.* Visual acuity after retinal gene therapy for choroideremia. *N Engl J Med* 2016;374:1996–8.
- Barnard AR, Groppa M, MacLaren RE. Gene therapy for choroideremia using an adeno-associated viral (AAV) vector. *Cold Spring Harb Perspect Med* 2014;5:a017293.
- Munk MR, Giannakaki-Zimmermann H, Berger L, *et al.* OCT angiography: a qualitative and quantitative comparison of 4 OCTA devices. *PLoS One* 2017;12:e0177059.